PROCEEDINGS, 42nd Workshop on Geothermal Reservoir Engineering
Stanford University, Stanford, California, February 13-15, 2017
SGP-TR-212

Assessment of Sand-face Pressure and Temperature Behaviors of Single-Phase Liquid-Water Geothermal Reservoirs during Injection and Falloff Tests

Yildiray Palabiyik[1], Murat Cinar[1], Ihsan Murat Gok[1] and Mustafa Onur[2]

[1]Department of Petroleum and Natural Gas Engineering, Istanbul Technical University, Maslak, 34469, Istanbul, Turkey

[2]McDougall School of Petroleum Engineering, The University of Tulsa, Stephenson Hall 2335, Tulsa, OK, 74104, USA

palabiyiky@itu.edu.tr, cinarmura@itu.edu.tr, ihsan_murat_gok@hotmail.com, mustafa-onur@utulsa.edu

Keywords: sand-face pressure and temperature, 2D (*r-z*) non-isothermal model, reservoir parameters, sensitivity, injection/falloff.

ABSTRACT

This study focuses on the evaluation of sand-face pressure and temperature behaviors during cold water injection into single-phase liquid-water geothermal reservoir and a falloff period following the injection. In recent years, important technological developments (higher resolutions and better accuracy) in temperature gauges have made temperature data valuable in addition to pressure to obtain precious reservoir information data that could not be obtained from pressure data alone by history matching. From this point of view, some cases including different injection/falloff and variable-rate injection scenarios are taken into consideration in this study to be able to understand some interesting pressure and temperature responses arising from colder water injection into a hotter geothermal reservoir and study the sensitivities of various rock parameters (porosity, permeability, skin, and thermal conductivity) to the temperature in a fully-penetrated vertical well or to the pressure and temperature at an observation point (probe) along the wellbore for an homogeneous or anisotropic reservoir during those modes. In this work, a 2D (*r-z*) non-isothermal in-house simulator verified by commonly used two thermal reservoir simulators, which can also model some important mechanisms such as Joule-Thomson effects (heating/cooling), transient adiabatic fluid expansion/compression, convection, and conduction, have been used to investigate the aforementioned behaviors. In this study, thermal effects taken place by the cold water injection into the hot reservoir on the sand-face pressure are explained in detail and verified by some analytical expressions available in the literature. It has been revealed that density and mobility differences that cold water injected and original geothermal reservoir fluid have cause those effects. Hence the sand-face pressure exhibits interesting behaviors depending on the outer reservoir boundary condition (infinite-acting, insulated, and Dirichlet) considered as well. According to the sensitivities of various rock properties to the sand-face temperature, it has been observed that particularly falloff period may contain valuable information about some reservoir parameters such as permeability, skin, and thermal conductivity to take into account those in history matching. Additionally, it is possible to state that increasing skin enhances the temperature change at the sand-face in relation to the more pressure drop and skin effect on temperature is more pronounced during falloff period compared to injection.

1. INTRODUCTION

Although temperature data have been routinely recorded in well test applications along with pressure data from the past to present, they have been ignored to use for estimating reservoir properties and/or to make use of characterization purposes until last years. Today, as reported in some previous studies (Duru and Horne, 2011a; Al-Nhadi et al., 2014; Sidorova et al., 2015), it has been seen that it is possible to measure temperature with a better resolution than 0.01 K (0.01 ^{o}C) whereas technological deficiencies in the past related to temperature gauges limited the scientists dealing with petroleum and/or geothermal reservoir engineering to usage of only pressure data for the purposes mentioned above. Therefore, it has been recently noticed that using temperature data along with pressure data could provide valuable reservoir information that cannot be obtained by history matching pressure data alone as well as the effects of recent technological improvements and studies stated above about temperature metrology. All those progresses regarding this topic have encouraged various researchers including us to further investigate especially sand-face temperature behavior to figure out whether it is sensitive to which reservoir parameter(s). For this purpose, various injection (constant- or variable-rate) and falloff cases have been taken into consideration in this study.

In petroleum and geothermal reservoir engineering literature, it is possible to find numerous studies including analytical, semi-analytical, and numerical solutions suggested for modeling responses of sand-face temperature resulting from non-isothermal fluid flow in porous media (App, 2009, 2010, 2015a, 2015b; App and Yoshioka, 2013; Atkinson and Ramey (1972); Chekalyuk, 1965; Duru and Horne, 2010a, 2010b, 2011a, 2011b; Garg and Pritchett, 1977, 1984; Lauwerier, 1955; Onur and Cinar, 2016; Onur and Palabiyik, 2015; Onur et al., 2016; Palabiyik, 2013; Palabiyik et al., 2013, 2015; Palabiyik et al., 2016; Ramazanov and Nagimov, 2007; Ramazanov et al., 2010; Sidorova et al., 2015; Sui et al., 2008a, 2008b, 2010). All those studies including ours stated above make the assumption of local thermal equilibrium that means that solid rock phase and accompanying fluid phase in porous media are at the same temperature and that can be considered as a generally valid assumption to model thermal energy balance in most of the petroleum and geothermal reservoir systems.

This work primarily deals with the reservoir information content to be investigated by means of sand-face pressure and temperature responses arising from cold water injection into single-phase liquid-water geothermal reservoir and then, during a falloff period following the injection. For that purpose, various injection/falloff and variable-rate injection schemes are considered. The main goal of

this research is to seek the effects of some important reservoir parameters (porosity, permeability, skin, and thermal conductivity) on especially sand-face temperature behavior during different injection and falloff cases. To be able to support and quantify the understanding of the effects of those parameters on sand-face temperature, temporal sensitivity analyses are also performed by using the sensitivity coefficients to the temperature at an observation point (probe) along the wellbore in an homogeneous and anisotropic reservoirs during those modes mentioned above. Furthermore, thermal effects that are occurred by the cold water injection into a single-phase liquid-water geothermal reservoir on the sand-face pressure are studied for different outer reservoir boundary conditions in detail with this study and verified by an analytical solution improved by Bratvold and Horne (1990). Therefore, a 2-D (*r-z*) non-isothermal in-house simulator developed by Palabiyik (2013), Palabiyik et al. (2013; 2015; 2016) is used to accomplish all those cases stated above.

In the organization of the paper, firstly, the numerical model used is concisely introduced in the next section. Secondly, the case studies that contain different injection and falloff scenarios run by the 2-D (*r-z*) non-isothermal simulator are illustrated and explained in detail.

2. NUMERICAL MODEL USED IN CASES

The numerical simulator used in this study rigorously couples pressure diffusion and thermal energy balance equations by treating pressure and temperature dependent terms (rock, fluid, and thermal parameters) as a function of time and considering important mechanisms such as Joule-Thomson effects (heating/cooling), transient adiabatic fluid expansion/compression, convection, and conduction for single-phase liquid-water geothermal reservoirs. Darcy's law has been used to model the fluid velocity in the *r*- and *-z*-directions in convection term of the pressure diffusion equation. The non-linear model equations are solved in a fully-implicit approach by using a finite difference technique and the well-known Newton-Raphson's method. Different outer reservoir boundary conditions (infinite-acting, insulated, no-flow, no-heat flux, Dirichlet, etc.) related to pressure and temperature can be handled with the model. It can take heat transfer from reservoir to adjacent strata (over-burden and under-burden) via conduction and gravity effects in the *z*-direction into account. It is possible to model various production/injection schemes including buildup/falloff periods or variable-rate case histories as well. Rock properties (specific heat capacity, density, thermal conductivity, thermal expansion coefficient, compressibility and bulk volume) are assumed to be constant. All the details regarding the construction of the numerical model and its verification with the well-known commercial simulators TOUGH2 of Pruess et al. (1999), CMG-STARS (2015), and analytical solutions for different production and injection cases can be reached from Palabiyik (2013), Palabiyik et al. (2013; 2016)'s studies.

3. INJECTION/FALLOFF APPLICATIONS

In this section, the effects of various reservoir parameters and different well completion types (fully penetrating and limited-entry vertical wells) on sand-face pressure and temperature responses are investigated and interpreted through cold water injection into a single-phase liquid-water geothermal reservoir by using the 2-D (*r-z*) non-isothermal reservoir simulator during different injection and falloff modes. Various synthetic cases including different injection/falloff schemes are performed depending on different outer reservoir boundary conditions (ORBCs) in terms of pressure and temperature (infinite-acting, insulated, and Dirichlet types) given in Table 1.

Table 1: Outer reservoir boundary conditions (ORBCs).

Type of ORBC	p	T
Infinite-acting	$\lim_{r\to\infty} p(r,t) = p_o$	$\lim_{r\to\infty} T(r,t) = T_o$
Insulated	$\frac{\partial p}{\partial r}(r = r_e, t) = 0$	$T\,(r = r_e,\, t) = T_o$
Dirichlet	$p\,(r = r_e,\, t) = p_o$	$T\,(r = r_e,\, t) = T_o$

Uniform pressure and temperature distributions are taken into consideration in the reservoir as the initial conditions. We make an assumption of a horizontal reservoir to ignore gravity effects in the *z*-direction and heat transfer from reservoir to adjacent strata (at $z = 0$ and $z = h$) via conduction is also neglected in our application cases. The wells in which we have performed injection are assumed to be vertical. In all cases, homogeneous porosity and permeability distributions are considered and reservoirs are assumed isotropic unless otherwise mentioned. Since our research is mainly related to the sand-face pressure and temperature behaviors and studying the effects of wellbore storage is beyond the scope of this paper, the wellbore volume is assumed so small (approximately zero) to get rid of the wellbore storage effects. We also assume that there is no any dissolved solid in the geothermal fluid. In order that the simulated pressure and temperature values correspond to the sand-face ones, they are obtained at the midpoint perforations or just above the pay zone for both fully-penetrating and limited-entry vertical wells. The other related input reservoir properties with their definitions and values are presented in Table 2.

3.1 Effects of Permeability and Skin on Sand-face Temperature during Injection and Falloff

In these cases, the effects of changing permeability and skin on the sand-face temperature are investigated during injection and falloff periods. At first, water having the temperature of 333.15 K (60 ^{o}C) is injected from a fully penetrating vertical well into the single-phase liquid-water geothermal reservoir having the initial reservoir temperature of 423.15 (150 ^{o}C) at a constant-rate of 40 kg/s during 5 days (120 h) and then, the well is shut-in during the period of 20.83 days (500 h) following the injection. In practice, although a period of 500 h looks like a little bit longer time for a typical falloff application, we think that it could be important to clearly demonstrate the effects of permeability and skin on the sand-face temperature behavior during particularly falloff period. The reservoir radius has been chosen as a very large distance (r_e = 25000 m) to provide the infinite-acting ORBC (the 2nd row in Table 1) for our applications here. The well-

known Hawkins' formula has been used for the skin cases. Input data that contain reservoir parameters used in this case are given in Table 2.

Table 2: Input data for the Case 3.1.

Parameter	Definition of Parameter	Value
p_o, kPa	Initial reservoir pressure	12500
T_o, K	Initial reservoir temperature	423.15
T_{inj}, K	Temperature of injected water	333.15
r_w, m	Well radius	0.1
r_e, m	Reservoir radius	25000
h, m	Reservoir thickness	50
ϕ	Reservoir porosity	0.1
k, m^2	Absolute reservoir permeability	4.94×10^{-14}
S	Skin factor	0
c_s, 1/kPa	Isothermal compressibility of rock	2.9×10^{-7}
β_s, 1/K	Isobaric thermal expansion coefficient of rock	0
$c_{p,s}$, J/kgK	Specific heat capacity of rock	1000
ρ_s, kg/m^3	Density of solid rock phase	2650
λ_t, J/msK	Total thermal conductivity	3.12

Figures 1 and 2 show the effects of permeability and skin on the sand-face temperature during injection period, respectively. As can be seen from the figures, permeability or skin, no matter what their values are, does not affect the sand-face temperature during injection period. On the other hand, shown in Figures 3 and 4 are the effects of permeability and skin on the sand-face temperature during falloff period. According to Figure 3, we observe the largest sand-face temperature change in the reservoir with the lowest permeability of 1 md (9.87×10^{-16} m^2) because the biggest pressure increase has been experienced in this reservoir during the injection period before the following falloff period. For this reason, the sand-face pressure starts going down to balance the pressure increase taking place during the injection after the well is shut-in. At the beginning of the falloff (at very early time), the sand-face temperature decreases with the transient effect of adiabatic expansion. Then, the J-T effect surpassing the transient adiabatic expansion heats up the sand-face temperature until the end of the falloff. As can be seen from Figure 3, temperature change is remarkable especially for the reservoirs with very low permeability. As for the Figure 4, the mechanisms occurring at the sand-face are very similar to the permeability case. In this case, we observe the greatest sand-face temperature change in the reservoir with the highest skin because the largest resistance to flow in the vicinity of the well and the most pressure increase due to this resistance has been seen in this reservoir during the injection period. At the falloff following the injection, firstly, the transient adiabatic expansion causes a decrease in temperature at the sand-face, secondly, the J-T effect creates the largest temperature increase by dominating over the transient adiabatic expansion particularly in the reservoir with the highest skin.

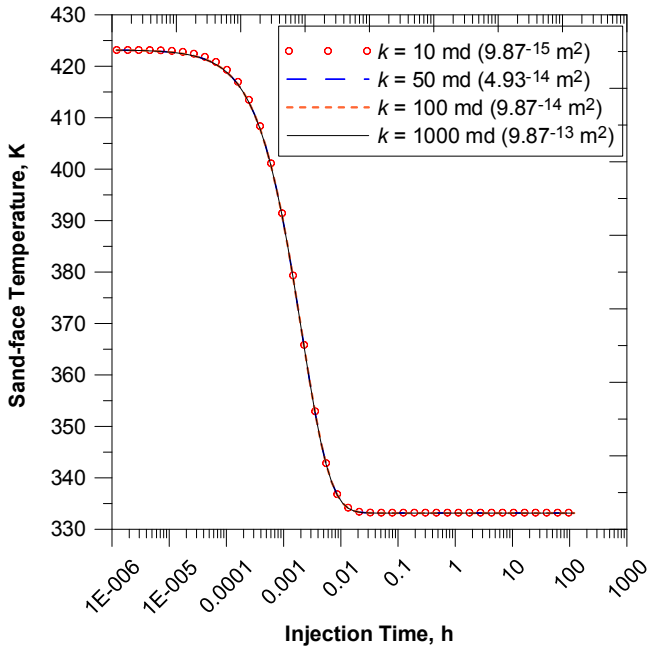

Figure 1: Effects of permeability on the sand-face temperature during injection from a fully penetrating well.

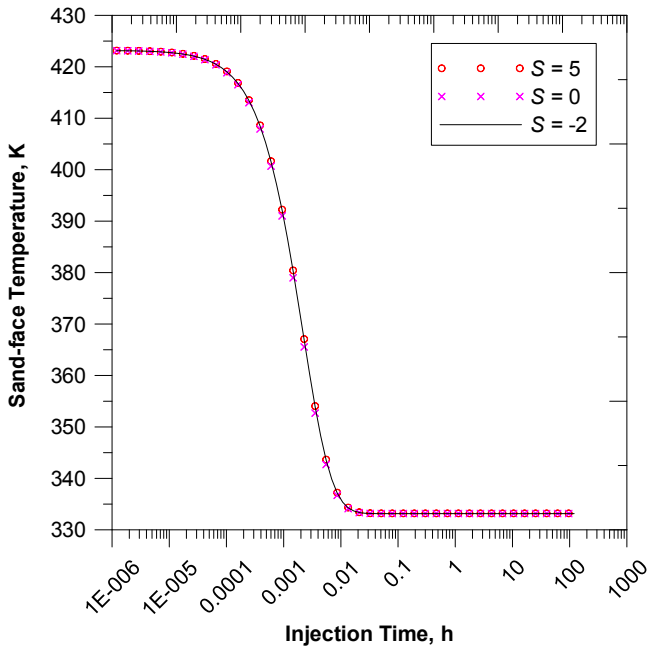

Figure 2: Effects of skin on the sand-face temperature during injection from a fully penetrating well.

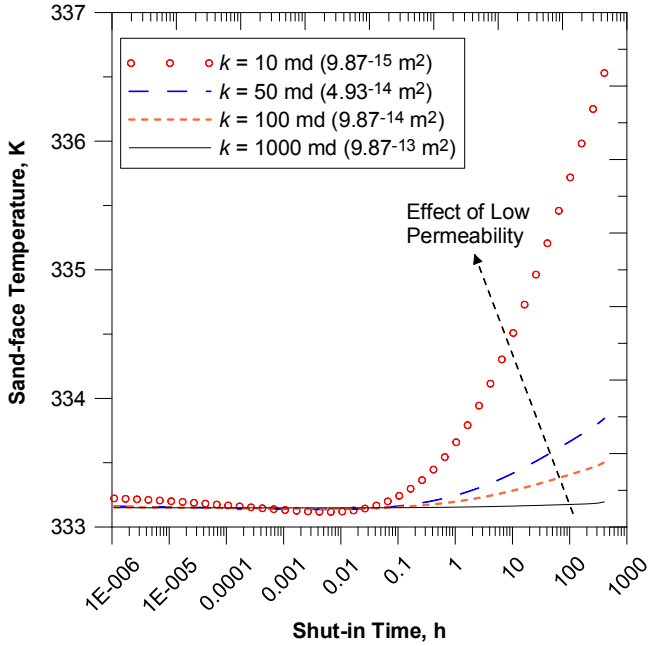

Figure 3: Effects of permeability on the sand-face temperature during falloff period for a fully penetrating well.

3.2 Effects of Different ORBC Types on Sand-face Pressure during Injection

In this case, the effects of different ORBC types [insulated (the 3rd row in Table 1) and Dirichlet (the 4th row in Table 1)] on the sand-face pressure are investigated during injection period. Water having the temperature of 333.15 K (60 °C) is injected from a fully penetrating vertical well into the single-phase liquid-water geothermal reservoir having initial reservoir temperature of 413.15 (140 °C) at a constant-rate of 1 kg/s during 1000 days. Figure 5 illustrates that the reservoir is to be surrounded by a huge edge aquifer to have a Dirichlet type ORBC. Input reservoir and aquifer data used in this case are presented in Table 3.

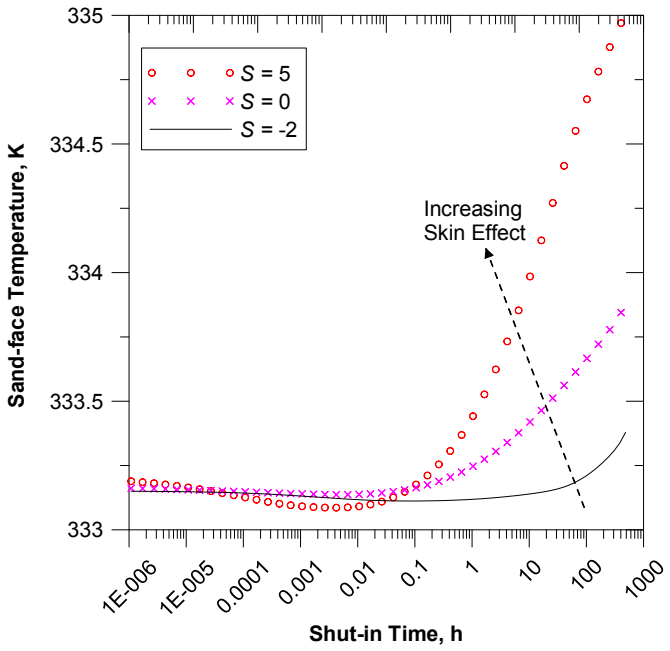

Figure 4: Effects of skin on the sand-face temperature during falloff period for a fully penetrating well.

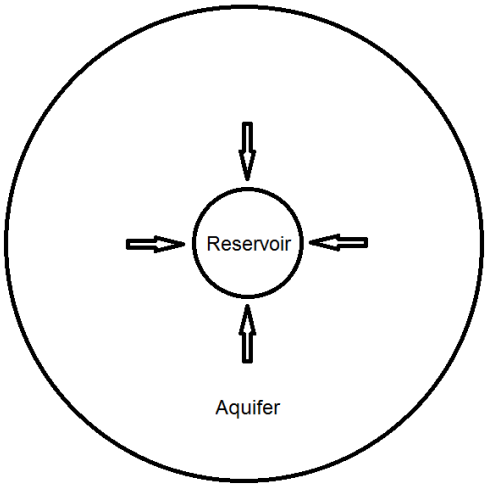

Figure 5: Schematic of a huge edge aquifer surrounding the reservoir from the top view.

Figure 6 shows the log-log diagnostic plots of sand-face pressure change and their Bourdet derivatives defined as the derivative of the sand-face pressure change with respect to the natural logarithm of time, that is, $\Delta p' = d\Delta p/d\ln t$ (Bourdet et al., 1989) as a function of time during at a constant-rate injection of 1 kg/s from fully penetrating well during 1000 days for insulated and Dirichlet types of ORBCs. Insulated ORBC has also been included into the case to clearly make a comparison between two different ORBC types and put forward the effect of Dirichlet ORBC on the sand-face pressure. A much cooler water having higher viscosity and density than those of the original geothermal reservoir water is injected into the reservoir in this case. Firstly, we observe the first radial flow period that the original hotter reservoir fluid dominates. After this duration, a constant derivative line where the first radial flow period is observed to exhibit an increasing derivative trend. This is because the cold water zone in the reservoir created by the injected fluid is still moving and the new injected cold fluid is coming across with the cold water zone previously created in the reservoir. Finally, we see that the unit slope line of the Bourdet derivative which points out a sealed outer boundary and so, a pseudo steady-state flow regime is experienced for the insulated ORBC since the outer boundary of the reservoir feels the pressure signal propagating throughout the reservoir before seeing the second radial flow regime dominated by the colder fluid injected into the reservoir. On the other hand, we

cannot observe the steady-state flow for the Dirichlet ORBC during the injection period because a resistance to injection occurs and makes very difficult to displace the cold fluid front having higher viscosity and density. Although it is not shown here, the steady-state flow would be observed if the period was extended to 10^6 days (practically an impossible duration). Furthermore, it is possible to observe another constant derivative line at late time for the Dirichlet ORBC case. It is interesting that the value of this derivative line at late time is greater than that of the first derivative line at early time that indicates the mobility of the hotter original reservoir fluid. Bratvold and Horne (1990) observed the same behavior in a similar problem that cold water injection has been performed into a hot oil reservoir with constant-pressure outer boundary and derived an analytical equation for this late-time constant-derivative (zero-slope) line, which can be given as follows:

Table 3: Input data for the Case 3.2.

Parameter	Definition of Parameter	Value
p_o, kPa	Initial reservoir pressure	10000
T_o, K	Initial reservoir temperature	413.15
T_{inj}, K	Temperature of injected water	333.15
r_w, m	Well radius	0.1
r_e, m	Reservoir radius	1000
h, m	Reservoir thickness	100
$V_{b,aq}$, m^3	Bulk volume of aquifer	10^{99}
ϕ	Porosity of reservoir and aquifer	0.2
k, m^2	Absolute reservoir permeability	1×10^{-13}
S	Skin factor	0
c_s, 1/kPa	Isothermal compressibility of rock	2.9×10^{-7}
β_s, 1/K	Isobaric thermal expansion coefficient of rock	0
$c_{p,s}$, J/kgK	Specific heat capacity of rock	1000
ρ_s, kg/m^3	Density of solid rock phase	2650
λ_t, J/msK	Total thermal conductivity	2.92

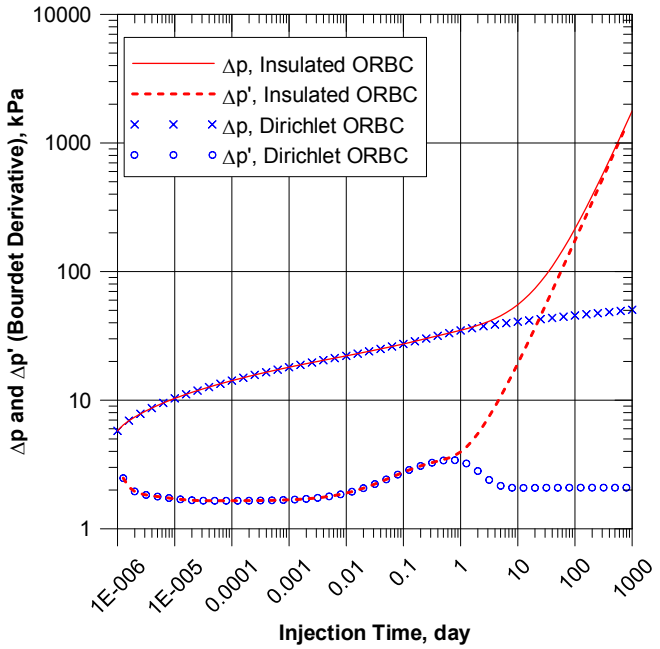

Figure 6: Effects of different ORBC types on sand-face pressure during injection from a fully penetrating well.

$$p_D' = 0.5(1-M) \tag{1}$$

In Eq. 1, p_D' represents dimensionless pressure derivative based on the mobility of the injected water and M represents the mobility ratio. In our case, M represents the ratio of the mobility of injected colder water to the mobility of the hotter reservoir water. Since our case considered here is the flow of a single-phase liquid-water in a homogeneous reservoir, then M in Eq. 1 only depends on the ratio of the viscosity of the original reservoir fluid to the viscosity of the injected fluid and the new equality can be expressed as follows:

$$p_D^{'} = 0.5\left(1 - \frac{\frac{k}{\mu_{w,inj}}}{\frac{k}{\mu_{w,res}}}\right) = 0.5\left(1 - \frac{\mu_{w,res}}{\mu_{w,inj}}\right) \tag{2}$$

If the pertinent viscosity values ($\mu_{w,res}$ = 0.000199 Pa.s and $\mu_{w,inj}$ = 0.000469 Pa.s) are inserted into Eq. 2, the dimensionless pressure-derivative value for the late-time solution can be computed as follows:

$$p_D^{'} = 0.5\left(1 - \frac{0.000199}{0.000469}\right) \tag{3}$$

$$p_D^{'} = 0.288 \tag{4}$$

The dimensionless pressure-derivative $p_D^{'}$ can also be defined by the following equation in SI units:

$$p_D^{'} = \frac{2\pi kh}{q\mu_{w,inj}}\Delta p' \tag{5}$$

where $\Delta p^{'}$ is the Bourdet derivative of the sand-face pressure change.

If the parameters, $k = 1\times10^{-13}$ m^2, h = 100 m, $q = 1.017\times10^{-3}$ m^3/s (volumetric flow rate), $\mu_{w,inj}$ = 0.000469 Pa.s, and $\Delta p^{'}$ = 2090.6 Pa, where $\Delta p^{'}$ is read from the constant-derivative line at late time for the Dirichlet ORBC case in Figure 6, are used in Eq. 5, the dimensionless-pressure derivative can be computed as follows:

$$p_D^{'} = \frac{2\times\pi\times10^{-13}\times100}{1.017\times10^{-3}\times0.000469}\times2090.6 \tag{6}$$

$$p_D^{'} = 0.275 \tag{7}$$

which matches very well with the value in Eq. 4.

3.3 Temperature sensitivity analysis at an observation point along wellbore during injection and falloff for a limited-entry well

In this subsection, the temperature behaviors are investigated at an observation (probe) point along the wellbore represented by a dual-packer configuration. Schematic of this configuration is shown in Figure 7. Injection is performed through the limited-entry well from the bottom of the reservoir where the pay zone has been located. These types of tests performed to acquire pressure and temperature measurements at the probe and dual-packer locations are generally applied for wireline formation testing if any vertical interference exists in the formation. Besides, they can be used for predicting horizontal and vertical permeability along with initial formation pressure and temperature and eventually obtaining in situ fluid samples for PVT analysis.

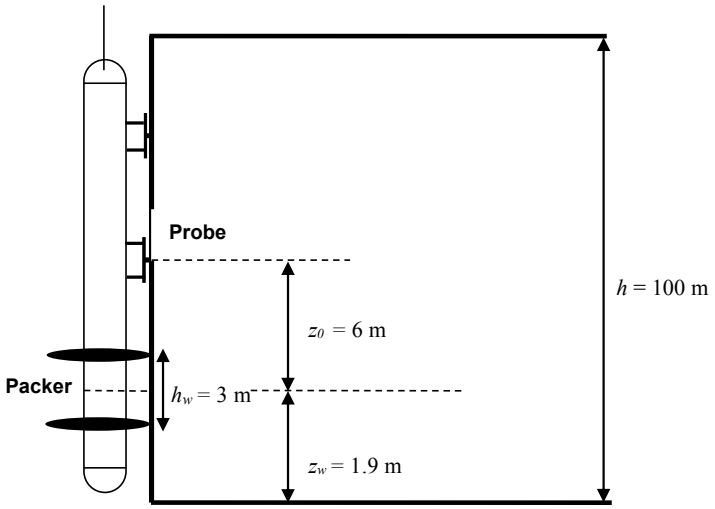

Figure 7: Demonstration of a probe configuration of a packer-probe wireline formation tester for a limited-entry vertical well.

These cases consist of injection-falloff tests that each one covers an injection period of 10 days (240 h) and a shut-in period of another 10 days (240 h) following the injection. Three different anisotropic reservoirs are considered. The reservoir in the first case has the horizontal permeability of $k_r = 1\times10^{-14}$ m^2 and the vertical permeability of $k_z = 1\times10^{-13}$ m^2 (anisotropy ratio = 0.1). The second one has a configuration of $k_r = 1\times10^{-13}$ m^2 and of $k_z = 1\times10^{-13}$ m^2 (anisotropy ratio = 1). The last one has a configuration of $k_r = 1\times10^{-12}$ m^2 and $k_z = 1\times10^{-13}$ m^2 (anisotropy ratio = 10). The other input parameters are the same as the Case 3.2. In these cases, the probe temperature sensitivities to various rock parameters are investigated by making use of the temporal sensitivity coefficient plots. Sensitivity coefficient ($\underline{S}$) of a primary variable (ψ) (temperature in our cases) with respect to the natural logarithm of a model parameter (κ) (such as porosity) can be defined as follows (the units of the sensitivity coefficients are K which gives us an opportunity to conveniently compare the sensitivity coefficients of different parameters with each other in a single figure):

$$\underline{S} = \left(\frac{\partial \psi}{\partial \ln \kappa}\right) = \kappa\left(\frac{\partial \psi}{\partial \kappa}\right) \tag{8}$$

Figure 8 shows the sensitivities of the probe temperature to some rock parameters (porosity, horizontal and vertical permeability, and thermal conductivity) for the reservoir with $k_r = 1\times10^{-14}$ m^2 and $k_z = 1\times10^{-13}$ m^2 as a function of injection time. We can see from Figure 8 that the probe temperature does not indicate any sensitivity to any rock parameter during injection until the colder front reaches the probe (approximately 2 h). After this occurs, the sensitivities of the probe temperature to the parameters start increasing with further propagation of the cold front. At late time of injection, the cold front completely reaches the probe and the sensitivities starts decreasing by the end of the injection period and eventually approximate to zero because any temperature change does not take place at the probe anymore. It is obvious from Figure 8 that the probe temperature indicates the largest and the same magnitude of sensitivity to both horizontal and vertical permeability. Nevertheless, the sensitivity to vertical permeability is negative whereas the sensitivity to horizontal one is positive. This means that the sensitivity of the probe temperature is inversely proportional to the vertical permeability while it is directly proportional to the horizontal one. The probe temperature is less sensitive to thermal conductivity and porosity than the permeability and shows positive sensitivity to those parameters during injection. Figure 9 shows the probe temperature's sensitivities during falloff following the injection for the same case. The probe temperature shows the greatest sensitivity to thermal conductivity at fall-off period and this sensitivity increases by the end of the falloff. This is expected because the falloff period is known as a conduction dominated period. Furthermore, the injection has been performed from the bottom of the reservoir and vertical permeability is ten times greater than the horizontal one. Conduction is much slower mechanism than convection and temperature variation (increase) supported by the surroundings of the probe, hotter parts of the reservoir, lately occurs during the falloff compared to the temperature change (decrease) at the probe taking place at the injection. Hence, at the falloff, one can observe this increase in sensitivity to thermal conductivity later than the injection. On the other hand, horizontal and vertical permeability exhibit an inverse sensitivity trend especially to the end of the falloff compared to the injection as expected.

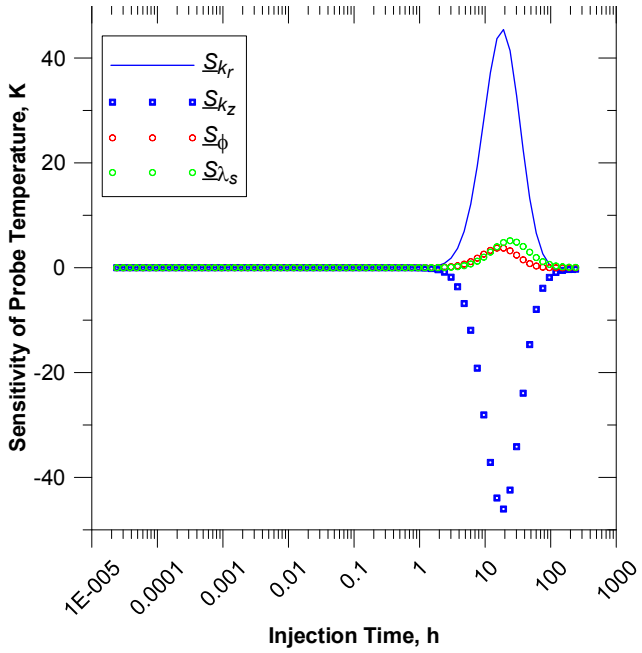

Figure 8: Sensitivities of the probe temperatures to the rock parameters during injection for the reservoir with an anisotropic configuration of $k_r = 1\times10^{-14}$ m^2 and $k_z = 1\times10^{-13}$ m^2.

Figure 10 shows the sensitivities of the probe temperature to the same rock parameters for the reservoir with $k_r = 1\times10^{-13}$ m^2 and $k_z = 1\times10^{-13}$ m^2 as a function of injection time. The probe temperature does not indicate any sensitivity to any rock parameter during injection until the colder front reaches the probe (approximately 10 h) as is in the previous case. Sensitivity reaction time at the probe

for this case shows up approximately 5 times later than the previous case because the horizontal permeability is 10 times greater than the previous one while the vertical permeability remains the same. Sensitivity behaviors are like the previous case except that they realize later. Figure 11 shows the sensitivities of the probe temperature during falloff for the same case. Although the probe temperature looks like to show the greatest sensitivities to the permeability, this is due to the delay taking place during the injection period. If the falloff period was extended to a duration long enough (even though generally not feasible and practical), one would probably observe that the greatest sensitivity had the thermal conductivity.

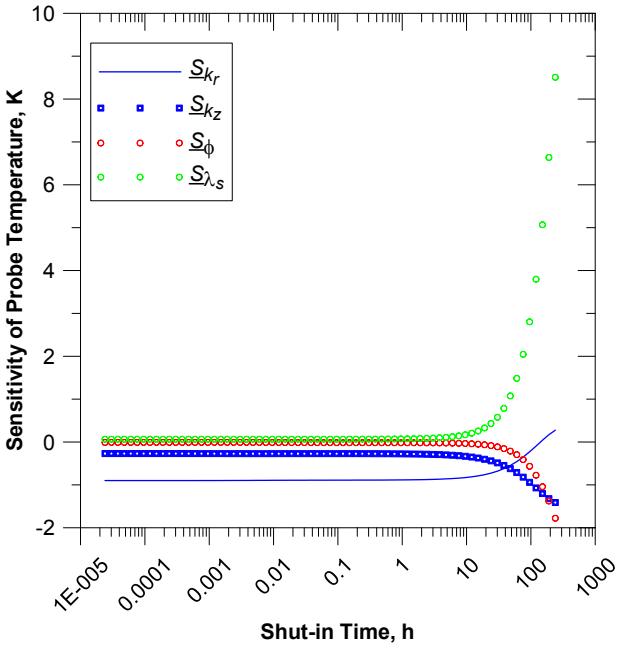

Figure 9: Sensitivities of the probe temperatures to the rock parameters during falloff for the reservoir with an anisotropic configuration of $k_r = 1\times10^{-14}$ m^2 and $k_z = 1\times10^{-13}$ m^2.

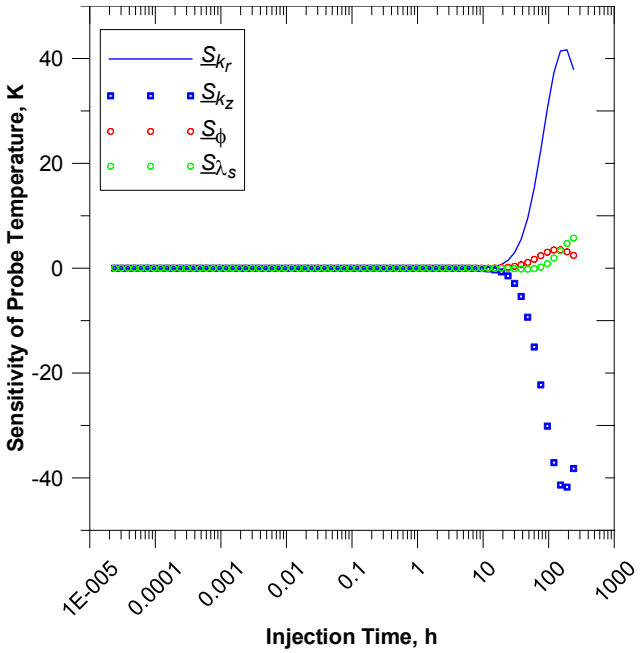

Figure 10: Sensitivities of the probe temperature to rock parameters during injection for the reservoir with an anisotropic configuration of $k_r = 1\times10^{-13}$ m^2 and $k_z = 1\times10^{-13}$ m^2.

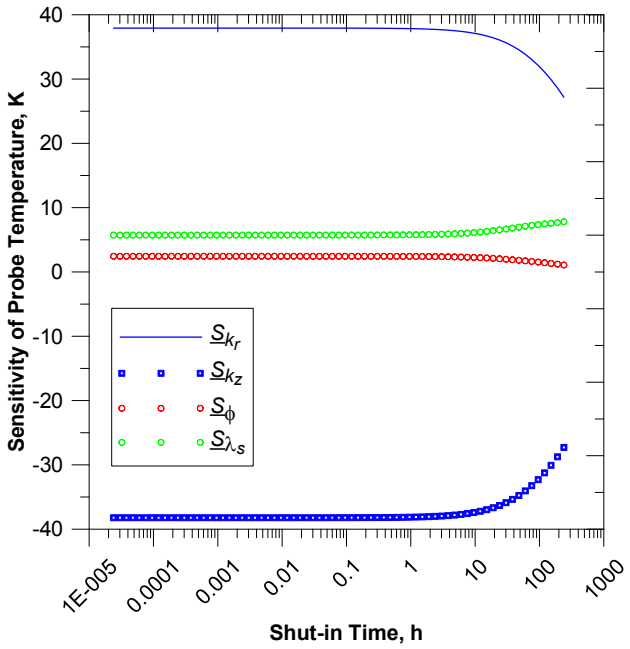

Figure 11: Sensitivities of the probe temperature to rock parameters during falloff for the reservoir with an anisotropic configuration of $k_r = 1\times10^{-13}$ m^2 and $k_z = 1\times10^{-13}$ m^2.

Figures 12 and 13 show the sensitivities of the probe temperature to the same rock parameters for the reservoir with $k_r = 1\times10^{-12}$ m^2 and $k_z = 1\times10^{-13}$ m^2 as a function of injection and shut-in times, respectively. The probe temperature does not indicate any sensitivity to any rock parameter during injection until the colder front reaches the probe (approximately 40 h) as is in the previous cases. Sensitivity reaction time at the probe for this case appears approximately 4 times later than the previous case because the horizontal permeability has the highest value among all the cases while the vertical permeability remains the same again. Differently from the previous cases, the probe temperature sensitivity to horizontal and vertical permeability is lower because resistance to flow in the *r*-direction goes down because of increasing horizontal permeability value.

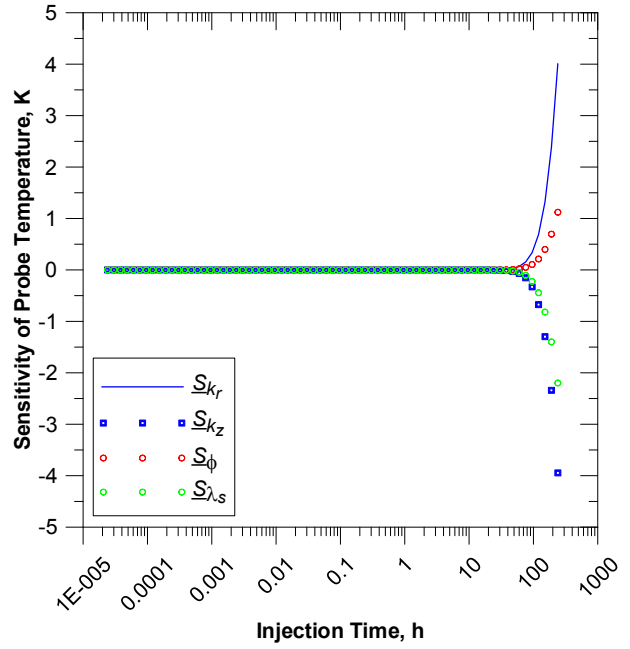

Figure 12: Sensitivities of the probe temperature to rock parameters during injection for the reservoir with an anisotropic configuration of $k_r = 1\times10^{-12}$ m^2 and $k_z = 1\times10^{-13}$ m^2.

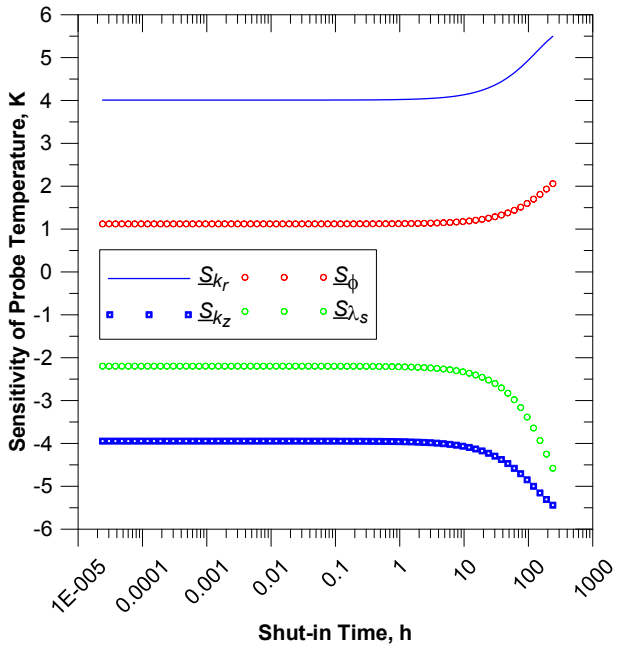

Figure 13: Sensitivities of the probe temperature to rock parameters during falloff for the reservoir with an anisotropic configuration of $k_r = 1\times10^{-12}$ m^2 and $k_z = 1\times10^{-13}$ m^2.

4. CONCLUDING REMARKS AND FUTURE WORKS

The sand-face temperature changes during shut-in period due to the combined J-T and transient adiabatic expansion effects of the fluid. At early times, the sand-face temperature decreases due to the transient adiabatic expansion whereas it increases due to the J-T effect surpassing the transient adiabatic expansion after early times.

It has been experienced that permeability and skin do not significantly affect the sand-face temperature during colder water injection from a fully penetrating vertical well into the single-phase liquid-water geothermal reservoir while the sand-face temperature may dramatically change with decreasing permeability or increasing skin values and this effect can be remarkable particularly for very low permeability and high skin values during shut-in period.

It has been observed that another constant (zero) Bourdet derivative-line will be experienced at late time during colder water injection from a fully penetrating vertical well into the single-phase liquid-water geothermal reservoir and the mobilities (or viscosities) of the cold water injected and the original geothermal water will play an important role in the observation such a pressure behavior at the sand-face if Dirichlet type outer reservoir boundary condition is used. This has also been verified by an analytical expression available in the literature.

In the temperature sensitivity analysis performed at an observation point (probe) along the wellbore above the pay zone during cold water injection from a limited-entry well, it has been experienced that the probe temperature shows the largest sensitivity to the horizontal and vertical permeability for the reservoir having $k_r = 1\times10^{-14}$ m^2 and $k_z = 1\times10^{-13}$ m^2 whereas it shows the greatest sensitivity to rock thermal conductivity during shut-in period. It has been seen that the response time of the probe temperature sensitivity to any rock parameter at the injection period is postponed with increasing anisotropy ratio (or increasing horizontal permeability by fixing the vertical permeability) and this affects the sensitivity behavior of the probe temperature during shut-in period as well.

As for the future works regarding these types of injection/falloff applications, the following studies can contribute to this research.

- Temporal sensitivity studies should be further investigated for different well completion types.
- 2-D (r-z) spatial sensitivity maps should be constructed as well as the temporal analyses to extend the research.
- Rate effect on the sand-face temperature behavior along with rock parameters should be studied.
- Wellbore storage effects on predicting rock parameters from the sand-face temperature can be investigated.
- Heat transfer effect from reservoir to adjacent strata on the sand-face and/or reservoir temperature can be studied.

ACKNOWLEDGEMENTS

We would like to thank the Scientific and Technological Research Council of Turkey (TUBITAK, Project No: 110M482) and the Unit of Istanbul Technical University (ITU) Scientific Research Projects to support this research financially. Some portions of this study come into existence of the PhD thesis of the first author.

REFERENCES

Al-Nhadi, A., Gill, H.S., Kumar, V., Karunakaran, P., and Azem, W.: Innovative Positioning of Downhole Pressure Gauges Close to Perforations in HPHT Slim Well during a Drillstem Test. Presented at the Offshore Technology Conference, Houston, Texas (2014). http://dx.doi.org/10.4043/25207-MS.

App, J.F.: Field Cases: Nonisothermal Behavior due to Joule-Thomson and Transient Fluid Expansion/Compression Effects, *Proceedings*, SPE Annual Technical Conference and Exhibition, SPE, New Orleans, Louisiana (2009). http://dx.doi.org/10.2118/124338-MS.

App, J.F.: Nonisothermal and Productivity Behavior of High Pressure Reservoirs, *SPE Journal*, **15**, (2010), 50-63.

App, J.F.: Influence of Flow Geometry on Sandface Temperatures during Single-Phase Oil Production: Dimensionless Analysis, *SPE Journal*, (2015a). http://dx.doi.org/ 10.2118/166298-PA.

App, J.F.: Permeability, Skin and Inflow Profile Estimation from Prodcution Logging Tool Temperature Traces, *Proceedings*, SPE Annual Technical Conference and Exhibition, SPE, Houston, Texas (2015b). http://dx.doi.org/10.2118/174910-MS.

App, J.F. and Yoshioka, K.: Impact of Reservoir Permeability on Flowing Sandface Temperatures: Dimensionless Analysis, *SPE Journal*, **18**, (2013), 685-694. http://dx.doi.org/ 10.2118/146951-PA.

Atkinson, P.G. and Ramey, H.J.Jr.: Problems of Heat Transfer in Porous Media, the 52nd SPE Annual Fall Technical Conference and Exhibition, Denver, CO (1972).

Bourdet, D., Ayoub, J.A., and Pirard, Y.M.: Use of Pressure Derivative in Well-Test Interpretation, *SPE Formation Evaluation*, **4**, (1989), 293-302.

Bratvold, R.B. and Horne, R.N.: Analysis of Pressure-Falloff Tests Following Cold-Water Injection, *SPE Formation Evaluation,* **5**, (1990), 293-302.

Chekalyuk, E.B.: Thermodynamics of Oil Formation (in Russian). Nedra, Moscow, Russia (1965).

CMG-STARS: Advanced Process and Thermal Reservoir Simulator v2015.10.5715.22942, Computer Modelling Group Ltd., Alberta, Canada (2015).

Duru, O.O. and Horne, R.N.: Modelling Reservoir Temperature Transients and Reservoir-Parameter Estimation Constrained to the Model, *SPE Reservoir Evaluation & Engineering*, **13**, (2010a), 873-883.

Duru, O.O. and Horne, R.N.: Joint Inversion of Temperature and Pressure Measurements for Estimation of Permeability and Porosity Fields, SPE Annual Technical Conference and Exhibition, Florence (2010b).

Duru, O.O. and Horne, R.N.: Simultaneous Interpretation of Pressure, Temperature, and Flow Rate Data Using Bayesian Inversion Methods, *SPE Reservoir Evaluation & Engineering*, **14**, (2011a), 225–238. http://dx.doi.org/10.2118/124827-PA.

Duru, O.O. and Horne, R.N.: Combined Temperature and Pressure Data Interpretation: Applications to Characterization of Near-Wellbore Reservoir Structures, SPE Annual Technical Conference and Exhibition, Denver, CO (2011b).

Garg, S.K. and Pritchett, J.W.: On Pressure-Work, Viscous Dissipation and the Energy Balance Relation for Geothermal Reservoirs, Adv. Water Resour., **1**, (1977), 41-47. http://dx.doi.org/10.1016/0309–1708(77)90007-0.

Garg, S.K. and Pritchett, J.W.: Pressure Transient Analysis for Hot Water Geothermal Wells, Rosenhein, J. and Bennett, G.D. (Eds.), Ground Water Hydraulics, Water Resources Monogr. 9, AGU, Washington, D.C., (1984), 242-255. http://dx.doi.org/10.1029/WM009p0242.

Lauwerier, H.A.: The Transport of Heat into an Oil Layer Caused by the Injection of Hot Fluid, *Journal of Applied Science Research*, **5**, (1955), 145-150.

Onur, M. and Cinar, M.: Temperature Transient Analysis of Slightly Compressible Single-Phase Reservoirs, *Proceedings*, SPE Europec Featured at 78th EAGE Conference and Exhibition, EAGE and SPE, Vienna, Austria (2016).

Onur, M. and Palabiyik, Y.: Nonlinear Parameter Estimation Based on History Matching of Temperature Measurements for Single-Phase Liquid-Water Geothermal Reservoirs, *Proceedings*, World Geothermal Congress, Melbourne, Australia (2015).

Onur, M., Palabiyik, Y., Tureyen, O.I., and Cinar, M.: Transient Temperature Behavior and Analysis of Single-Phase Liquid-Water Geothermal Reservoirs during Drawdown and Buildup Tests: Part II. Interpretation and Analysis Methodology with Applications, *Journal of Petroleum Science and Engineering*, **146**, (2016), 657-669. http://dx.doi.org/10.1016/j.petrol.2016.08.002.

Palabiyik, Y.: Pressure and Temperature Behaviors of Single-Phase Water Geothermal Reservoirs under Various Production/Injection Schemes, ITU Graduate School of Science Engineering and Technology, PhD (2013).

Palabiyik, Y., Tureyen, O.I., Onur, M., and Deniz, M.: A Study on Pressure and Temperature Behaviors of Geothermal Wells in Single-Phase Liquid Reservoirs, *Proceedings*, 38th Workshop on Geothermal Reservoir Engineering, Stanford University, Stanford, CA (2013).

Palabiyik, Y., Tureyen, O.I., and Onur, M.: Pressure and Temperature Behaviors of Single-Phase Liquid Water Geothermal Reservoirs under Various Production/Injection Schemes, *Proceedings*, World Geothermal Congress. Melbourne, Australia (2015).

Palabiyik, Y., Onur, M., Tureyen, O.I., and Cinar, M.: Transient Temperature Behavior and Analysis of Single-Phase Liquid-Water Geothermal Reservoirs during Drawdown and Buildup Tests: Part I. Theory, New Analytical and Approximate Solutions, *Journal of Petroleum Science and Engineering*, **146**, (2016), 637-656. http://dx.doi.org/ 10.1016/j.petrol.2016.08.003.

Pruess, K., Oldenburg, C., and Moridis, G.: Tough2 User's Guide Version 2.0, Report 476, LBNL-43134, Lawrence Berkeley National Laboratory, Berkeley, CA (1999).

Ramazanov, A.S. and Nagimov, V.M.: Analytical Model for the Calculation of Temperature Distribution in the Oil Reservoir during Unsteady Fluid Flow, Oil and Gas Business (2007).

Ramazanov, A.S., Valiullin, R.A., Sadretdinov A.A., Shako, V.V., Pimenov, V.P., Fedorov, V.N., and Belov, K.V.: Thermal Modeling for Characterization of Near Wellbore Zone and Zonal Allocation, SPE Russian Oil and Gas Technical Conference and Exhibition, Moscow (2010).

Sidorova, M., Shako, V., Pimenov, V., and Theuveny, B.: The Value of Transient Temperature Responses in Testing Operations, *Proceedings*, SPE Middle East Oil & Gas Show and Conference, SPE, Manama, Bahrain (2015). http://dx.doi.org/ 10.2118/172758-MS.

Sui, W., Zhu, D., Hill, A.D., and Ehlig-Economides, C.: Model for Transient Temperature and Pressure Behavior in Commingled Vertical Wells, SPE Russian Oil and Gas Technical Conference and Exhibition, Moscow (2008a).

Sui, W., Zhu, D., Hill, A.D., and Ehlig-Economides, C.: Determining Multilayer Formation Properties from Transient Temperature and Pressure Measurements, SPE Annual Technical Conference and Exhibition, Denver, CO (2008b).

Sui, W., Zhu, D., Hill, A.D., and Ehlig-Economides, C.: Determining Multilayer Formation Properties From Transient Temperature And Pressure Measurements in Commingled Gas Wells, *Proceedings*, CPS/SPE International Oil & Gas Conference and Exhibition, Beijing, China (2010). http://dx.doi.org/10.2118/131150-MS.